Reactive transport modeling in carbonate rocks: Single pore model

Priyanka Agrawal[*1], Amir Raoof[1], Oleg Iliev[2], Janou Koskamp[1] and Mariëtte Wolthers[1]
1. Department of Earth Sciences, Utrecht University, Utrecht, Netherlands,
2. Fraunhofer ITWM, Kaiserslautern, Germany
* Corresponding Author: p.agrawal@uu.nl

Abstract

In the present study, a reactive transport model is presented that simulates carbonic-acid induced calcite dissolution. This dissolution results in a moving-pore-boundary problem. COMSOL Multiphysics is used to couple chemistry, flow, transport and moving boundary physics. Each process is discussed in detail. The results are compared for different flow rate after injecting same number of pore volume. It is noted that a characteristic pore shape develops depending upon the flow rate. These different pore shapes will relate conductivity and volume change differently.

1. Introduction

Calcite is the main mineral found in carbonate rocks, which form significant hydrocarbon reservoirs and subsurface repositories for CO_2 sequestration (Roehl and Choquette, 1985). The injected CO_2 mixes with the reservoir fluid and disturbs the geochemical equilibrium, triggering calcite dissolution. Since calcite dissolution is a mass-transfer limited process in fluids with a pH below 4 (Plummer et. al., 1978) both fluid chemistry and flow velocity affect the dissolution rate. Different combinations of fluid chemistry and injection rate may therefore result in different evolution of porosity, permeability and dissolution patterns.

Many research efforts have focused on predicting the dissolution behavior of carbonate for different flow and reaction regimes. A number of experiments have listed the results of such mixing-induced dissolution for different reaction and transport regimes (Fredd and Fogler, 1999 and Luquot et.al, 2014). Also, a range of modeling schemes have been developed to imitate experiments through solving reactive transport on continuum (Golfier et. al., 2002) and pore scales (Nunes et. al., 2016 and Nogues et. al., 2013).

Calcite dissolution changes pore geometry and connectivity continuously; updating these parameters at every time step becomes an important part of numerical models. However, continuous update of porous media geometry is computationaly expensive. That is why dissolution induced pore geometry changes are accounted in continuum

models through porosity-permeability relationships (Golfier et. al., 2002). The most commonly used porosity-permeability relationship is derived from the Kozeny-Carman equation (Kozeny, 1927 and Carman, 1937) in connection with Darcy's law. This relates permeability (K) to porosity ($\emptyset$) via a power law $K \propto (\emptyset)^n$. The prediction of the value of exponent n is mostly based on experimental data (Luquot et. al., 2014) or pore network models (Nunes et. al., 2016 and Nogues et. al., 2013).

In the pore network models proposed by Nogues et. al., 2013, the pore geometry changes are reflected through modifying the pore-throat conductivity. They related conductivity evolution with changes in pore volume using a single relationship for the entire network. In fact, at a single pore scale, this relationship is the result of the pore shape development due to dissolution. Here we present the discussion on pore-shape evolution for different transport regimes.

In this study, a reactive transport model is presented which simulates the complex chemical reaction of carbonic-acid induced calcite dissolution and subsequent pore-geometry evolution at a single pore scale. We use COMSOL Multiphysics package 5.3 for the simulation. COMSOL utilizes the arbitary-Lagrangian Eulerian (ALE) method for the free-moving domain boundary. In the past, several studies with moving pore boundary have used COMSOL (Kumar, et.al., 2011 and Noorden Van T. L., 2009) but for relatively simple reaction rate law.

The structure of the paper is as follows. In section 2, we present the model equations for all the physics and chemistry. Section 3 deals with the numerical implementation in COMSOL. Section 4 presents results for a single pore with straight pore wall at different flow velocities. We provide conclusions in section 5.

2. Model Set-up

The model solves fluid flow, transport, reaction and moving boundary in a domain which at t = 0 is a 2D rectangle and represents a single pore in carbonate rocks. The length and width of the rectangular pore

is L=250µm and d=75 µm respectively. The following subsections discuss physics, chemistry and implementation in COMSOL. Due to the non-uniform dissolution, the width evolves in time and space, d=d(x,t), with d(x,0)=d.

2.1 Fluid flow model

The fluid velocities in pores are very small (i.e. Reynolds number Re = ρud/µ << 1) so the Stokes equation for incompressible flow is considered to compute the velocity field in the single pore:

$$\rho \frac{\partial u}{\partial t} + \nabla . p = \mu(\Delta u) \quad (1)$$

$$\nabla . u = 0 \quad (2)$$

where, u is the fluid velocity, p is pressure, ρ is the fluid density and µ is the fluid viscosity.

At the inlet, the velocity is imposed from Poiseuille distribution profile and the longitudinal component is defined as:

$$u = u_o * 4 * s * (1 - s) \quad (3)$$

u_o is the maximum velocity and s is a value from 0 to 1 along the width of the inlet. Fluid flow is transient to account for the geometry change induced by calcite dissolution. For this purpose, a dimensionless variable s is used in defining the parabolic velocity profile at inlet. With the changing inlet width, s is recalculated for the new width at each time step, so the boundary profile remains same. Constant pressure is applied at the outlet. Lateral boundaries of pore have no slip condition.

To follow the moving solid boundary (pore wall), a normal velocity component is defined for the fluid as equivalent to velocity component of pore wall.

2.2 Geochemical model

The dissolution of calcite in the presence of CO_2-saturated water includes a set of equilibrium reactions within an aqueous phase and reversible reaction at the surface.

Equilibrium reactions correspond to mixing of CO_2(gas) in water which generates weak carbonic acid and further dissociation into HCO_3^- and CO_3^{2-}. Along with this system, water speciation reaction is also considered as:

$$K_1: \ CO_2(gas) = CO_2(aq)$$

$$K_2: \ CO_2(aq) + H_2O = H^+ + HCO_3^-$$

$$K_3: \ HCO_3^- = H^+ + CO_3^{2-}$$

$$K_4: \ H_2O = H^+ + OH^-$$

where K_1, K_2, K_3, and K_4 are equilibrium constants of the reactions. At 25°C, K_1 = 3.41 X 10^{-2}, K_2 = 4.5 X 10^{-7}, K_3 = 4.78 X 10^{-11}, K_4 = 1 X 10^{-14} (Plummer and Busenberg, 1982).

Lateral boundaries of the pore are the fluid-solid interface where calcite dissolution reaction takes place as:

$$CaCO_3 (s) = Ca^{2+}(aq) + CO_3^{2-}(aq)$$

The rate of calcite dissolution has been described by Plummer et al. (1978.) He used pure calcite crystals to study the dissolution for a range of P_{CO_2} and temperature conditions. The dependency of dissolution rate on pH, CO_2 activity and saturation index of fluid is given as:

$$R_{calcite} \ [\text{mol m}^{-2} \text{ s}^{-1}] = (k_1 * a_{H^+} + k_2 * a_{CO_{2(aq)}} + k_3 * a_{H_2O}) * (1 - 10^{(2*SI/3)}) \quad (4)$$

where, k_1 = 5.11 X 10^{-4}, k_2 = 3.42 X 10^{-7} and k_3 = 1.19 X 10^{-9} at 25°C (Plummer et.al., 1978) are the reaction rate constants , a_{H^+}, $a_{CO_{2(aq)}}$, a_{H_2O} are the activity of hydrogen ion, aqueous CO_2 and H_2O and SI is saturation index of fluid defined as the ratio of the ion activity product (product of $a_{Ca^{2+}}$ and $a_{CO_3^{2-}}$) and K_{sp} (solubility constant of calcite i.e. $10^{-8.48}$) (Plummer and Busenberg, 1982).

The dependency of the rate on aqueous species concentration causes non-linearity in the presented system.

2.3 Transport model

The advection-diffusion-reaction equation for each species in solution is given as:

$$\frac{\partial c_i}{\partial t} + \nabla . (-D_i . \nabla c_i) + \nabla . (u . c_i) = R_i \quad (5)$$

u, c_i, D_i and R_i are fluid velocity, concentration of species i, diffusion coefficient of species i and reaction input of species i per unit volume. D_i for all species is used as 10^{-9} m^2.s. For now, we have neglected charge-based diffusion coefficient variations for bulk species.

At the inlet, the injecting solution is considered to be in equilibrium with a fixed value of P_{CO_2}. Depending upon this value, the concentration of all species was calculated in PhreeqC (Parkhurst and Appelo, 2013) using phreeqc.dat database. PhreeqC is a geochemical model for speciation, batch reactions and reactive-transport problems. Table 1 lists concentration of all species for the 2 initial solutions.

For time t=0, a fluid in equilibrium with calcite is present in the pore. The initial concentration of all species was calculated as per this condition using PhreeqC.

The inflow boundary condition is based on prescribing the total flux; more details are given in section 3.1. The outlet boundary is exposed to free exit condition for all species. The Inlet and the outlet boundaries are not reactive.

Species	Injecting Solution ($mol.m^{-3}$)	Intial solution inside pore ($mol.m^{-3}$)
P_{CO_2}	-1.5	-6.17
$CO_2(g)$	31.622	6.76×10^{-4}
$CO_2(aq)$	1.076	2.27×10^{-5}
CO_3^{-2}	4.79×10^{-8}	3.38×10^{-2}
HCO_3^-	2.20×10^{-2}	8.35×10^{-2}
H^+	2.20×10^{-2}	1.27×10^{-7}
OH^-	4.65×10^{-7}	8.35×10^{-2}
Ca^{+2}	0	0.117
pH	4.66	9.90

Table 1: Concentration of aqueous species in injecting and initial solution

To conserve the mass across solid-fluid interface, the total (diffusive plus convective) flux equal to the reactive flux, is defined for all bulk species such as:

$$-n.(-D_i.\nabla c + u.c_i) = R_{calcite} \quad (6)$$

where, D_i and c_i are diffusion coefficient and concentration of species i, $R_{calcite}$ [mol m^{-2} s^{-1}] is the surface reaction rate and u is the fluid velocity.

2.4 Pore geometry evolution model

The calcite dissolution induced pore geometry change is modeled using ALE method. Since the lateral boundaries of the domain (i.e. the pore walls) are the only reactive ones so the velocity is defined only for these boundaries. This velocity depends on the reaction rate of calcite as:

$$V_y = R_{calcite} * MV \quad (7)$$

where, Vy is the velocity component in y-direction defined at lateral boundary of pore, Rcalcite is reaction rate of calcite [mol m^{-2} s^{-1}] and MV is molar volume of calcite, i.e. 3.69×10^{-5} [$m^3.mol^{-1}$].

In fact, the normal component of the velocity has to be used in the interface condition above. However, having in mind that currently we are performing qualitative studies, we use Vy to make the grid update easier and faster.

3. Implementation in COMSOL

In order to simulate the above-mentioned processes in COMSOL, we used laminar flow physics, chemistry and surface reactions, transport of diluted species physics, and moving boundary physics. To get this highly coupled model run, we had implemented it as follows.

Transport of diluted species physics

At t>0, an injecting solution of very different composition (pH = 4.66) starts mixing with the initial solution in the pore (pH = 9.9, Table 1). Due to the large difference in the composition of these two solutions, a sharp concentration gradient front develops at the inlet. Also, high reaction rate may occur near the inlet. To avoid oscillations in numerical solution, we used a flux (Danckwerts) boundary condition at the inlet. This is a velocity based flux condition normal to boundary:

$$n.(-D_i.\nabla c + u.c_i) = u.c_{oi} \quad (8)$$

where, D_i and c_{oi} are Diffusion coefficient and initial concentration of species i and u is the fluid velocity.

Further on, in order to avoid instabilities, the jump composition at the inlet (from pH=9.9 in the channel to pH=4 at the inlet) is imposed gradually at a certain time interval. A step function (Figure 1) is defined which gradually in time changes the composition of the injecting solution from pH 9.9 to pH 4.

$$S(t) = \begin{cases} 0, & t < t1 \\ 0 - 1, & t1 < t < t2 \\ 1, & t > t2 \end{cases} \quad (9)$$

This step function has three defining parameters in COMSOL i.e. t3 (location time around which the function is symmetric), size of the transition zone and number of continuous derivatives i.e. 2 for Figure 1. t1 and t2 are calculated with these parameters. The value of t3 and transition zone is such as this transient period is present for same number of pore volume across different flow rates.

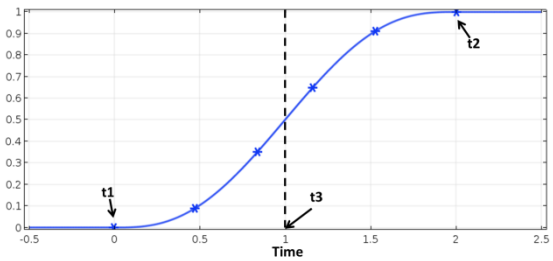

Figure 1: Step function defined for simulation done with maximum inlet velocity of 10^{-4} m/s. The value of t3 is 1s and transition zone size is 2s.

3.2 Mesh Statistics

In finite-element numerical methods, finer mesh makes the solution more accurate but also increases the computation time compared to coarse mesh. We carried out a mesh sensitive analysis and decided to use normal mesh in the bulk with the maximum element size of 3.38 µm and growth rate of 1.15. To acknowledge the moving boundaries (lateral boundary of pore) and the strong gradients due to mixing of two different fluids at inlet, we used a much finer triangular element along these boundaries. This has maximum element size of 2.49 µm and growth rate of 1.1. In total, the domain of 240 X 75 µm, has 6049 triangular elements with minimum element quality of 0.76.

3.3 Mesh quality study

The y-direction component of velocity at the lateral boundary of pore, induced by calcite dissolution, deforms the initially defined mesh. COMSOL provides an automatic re-meshing option which regenerates the mesh if the mesh quality becomes lower than the pre-defined threshold. This option is computationally expensive, so we checked the requirement for this option in our simulation time window. Figure 2 shows the original mesh and the deformed mesh after simulation time of 3 X 10^5 s, equivalent to 8000 pore volume numbers at maximum flow velocity 10^{-5} m/s. The color scale is for the mesh element quality index. This is the quotient of a mesh-element volume and the radius of a circle that circumscribes that particular mesh element. The value of this quality index is between 0 to1 with 0 being poor quality and 1 being perfect quality. For our system, the displacement is in order of µm so the mesh quality does not deteriorate below 0.5. The acceptable mesh quality threshold value is 0.1. So, for this simulation time, we did not need to use the automatic re-meshing option.

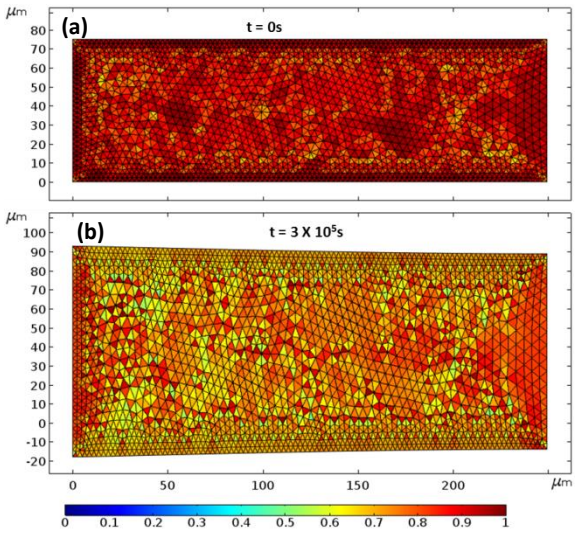

Figure 2: Mesh plot at (a) t = 0s and (b) t = 3 X10^5s showing the mesh element quality distribution

4. Results and Discussion

Each simulations was run until injecting the same total volume *V* which is equal to 8000 times the pore volume (PV) at t=0.

Pore Shape

The overall reaction rate of calcite dissolution depends on the rate of supply and removal of solute species to and from the reacting surface. To understand this dependency, we imposed different inflow rates, thereby achieving a flow range spanning from the diffusion controlled to the advection controlled transport regime. The Péclet number (Pe) is used to estimate the dominated processes, and it is defined as:

$$P_e = \frac{u_o * l}{D} \qquad (10)$$

where, u_o is maximum velocity at the center of the inlet, l is the half width of the original inlet and D is the diffusion coefficient. Note that the Pe number was calculated using the half width of inlet at t = 0s, even though this width changes with time.

Figure 3 shows the pore shapes after injecting 8000 PV numbers as changed from a rectangle at t = 0s. We present the simulated results for 3 Pe numbers: 3.75, 0.37, 0.037, which are analogous to a maximum inflow velocity of 10^{-4} m/s, 10^{-5} m/s and 10^{-6} m/s respectively. For each Pe number, 3 surfaces are shown such as velocity field, concentration of Ca and pH.

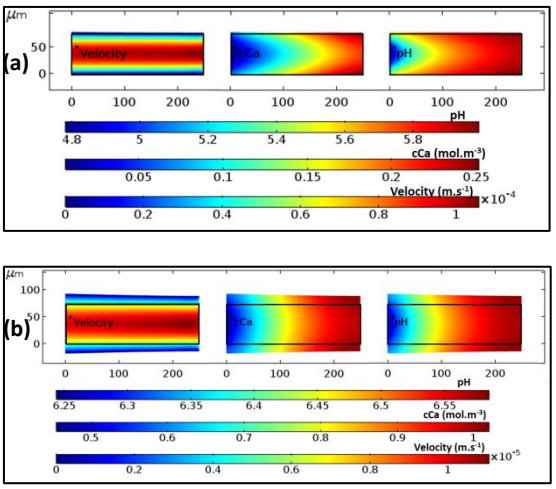

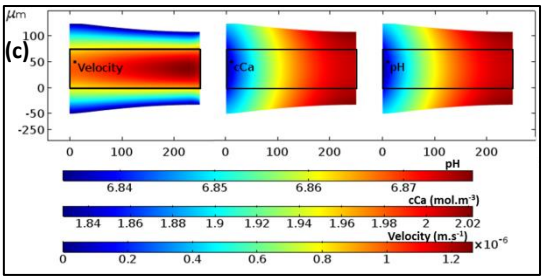

Figure 3: Simulation results to show different pore shape for different Pe numbers (a) 3.75, (b) 0.37 and (c) 0.037. For each Pe number, velocity (left pane), concentration of Ca (one of the reaction products, center pane) and pH profiles (right pane) are shown. The black rectangle within the profiles indicates the size of the pore at t=0s, the colored regions around the rectangle indicate zones dissolved during reaction.

We want to state following observations from these simulations:

a) Inlet boundary has a constant maximum velocity condition so the flux rate is changing due to increasing cross-section area at inlet. Figure 3 shows that the simulated inflow velocity field maintains the Poiseuille distribution as at t=0s, but with a different maximum value. This also results in an increasing high velocity zone at the outlet over the course of a simulation.

b) For the highest Pe number (3.75; Figure. 2a), the Ca^{2+} concentration and pH profile are following the parabolic velocity profile. This results in a transversal concentration gradient. However, with relatively low Pe numbers (0.37 and 0.037; Figure. 2b and c), diffusion reduces this transversal gradient.

c) The pH of the injecting flow is 4.66. Calcite dissolution increases the pH of the solution. From the pH profiles, we see that for Pe 3.75, pH buffering is less than for the lower Pe runs. This can be explained by insufficient time for mixing of reaction products into solution at higher flow rates. However, for relatively lower Pe 0.37 and 0.037, the inlet solution is buffered to a pH value of 6.35 and 6.85 respectively. This indicates that, after the same simulation time at high flow rate, the solution remains more reactive compared to slow flow rate (Figure 3). When considering the same number of pore volumes rather than the same simulation time, we observe more displacement of the pore boundary at Pe 0.0375

d) At high Pe number, the fluid remains reactive towards the calcite pore wall as it reaches towards the end of the pore due to the lower degree of buffering of the fluid. This means a similar reaction rate can be observed along the pore wall from inlet towards outlet. Eventually, this yields a uniform, near-linear pore-wall displacement due to uniform dissolution. Contrastingly, the slow-moving fluid is becoming more non-reactive by the time it reaches towards outlet due to continuous mixing and buffering by calcite dissolution. This results into lower dissolution rates at the outlet than inlet, yielding the non-uniform pore shapes shown in Figure 3b and 3c.

(e) To quantify the observations noted in the previous point, we computed the relative displacement for all Pe numbers as:

$$Y_{norm(x)} = \frac{Y_{inlet}}{Y_x}$$

where, Y_{inlet} and Y_x are the displacements at the inlet and at point x along the pore length, after injecting 8000 PV.

Figure 4 shows that the difference between the inlet and outlet displacement values increases as Pe number decreases.

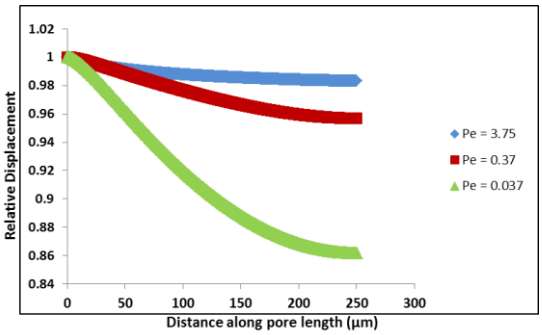

Figure 4: Relative displacement along pore length plotted for different peclet number after injection of same number of pore volumes (PV = 8000) for pH 4.66

(f) The pore shape discussed in previous points (d) and (e) are characteristic of each Pe number. These pore shapes are established after injection of some number of pore volumes and later the pore boundary moves normal to this established shape. Figure 5, shows the location of the top wall of the pore at two simulation times with respect to the original position for Pe number 3.75.

Figure 5 clearly shows that from 1000 sec onwards, the shape of the pore wall does not alter while the pore wall keeps retreating due to dissolution.

Such stable dissolution profiles are important for further relating the conductivity change with the pore volume change.

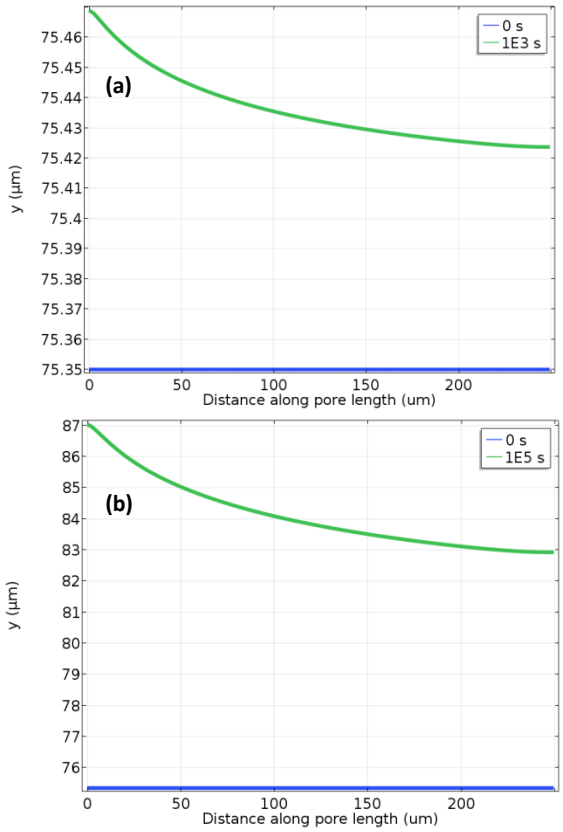

Figure 5: Position of top wall of the pore plotted at (a) t = 1000 s and 0s (b) t = 10^5s and t = 0s for Pe number 3.75

5. Summary and conclusions

In summary, we examined the effect of flow rate on the evolution of single pore shape profiles due to calcite dissolution. The flow field, surface and equilibrium reactions, solute transport and moving boundary were coupled in COMSOL Multiphysics software. We used three flow rates to cover diffusion dominated and advection dominated transport regimes. The fluid in diffusion dominated flow (Pe number 0.037 and 0.37) becomes less reactive along the pore length and thus produced non-uniform pore shapes. However, for the advection dominated flow (Pe number 3.75), the fast velocity of the fluid keeps the fluid relatively more reactive towards the end of the pore length, thus yielding uniform pore shape. Different pore shapes in terms of inlet opening vs overall pore opening, will have an impact on the relation between changing volumes and conductivity. Another conclusion from these simulations is that COMSOL can be used to solve complex chemistry, flow and moving boundary problems in the reactive transport domain.

References

1. Carman P., Fluid flow through granular beds, *Trans. Inst. Chem. Eng.* **15**, 150 (1937)

2. Fredd, C. N. and Fogler, H. S. Optimum conditions for wormhole formation in carbonate porous media: Influence of transport and reaction, *SPE Journal*, **4(3)**, 196–205 (1999)

3. Golfier, F., Zarcone, C., Bazin, B., Lenormand, R., Lasseux, D., Quintard, M. On the ability of a Darcy-scale model to capture wormhole formation during the dissolution of a porous medium, *J. Fluid Mech.*, **457**, 213–254 (2017)

4. Kumar, K., Van Noorden, T. L. and Pop, I. S. Effective dispersion equations for reactive flows involving free boundaries at the microscale, Multiscale Model. Simul., **9(1)**, 29–58 (2011)

5. Kozeny, J., Über die kapillare leitung des wassers im boden, *Sitz. Ber. Akad. Wiss. Wien, Math. Nat.* **136(2a)**, 271-306 (1927)

6. Luquot, L., Rodriguez, O. and Gouze, P. Experimental characterization of porosity structure and transport property changes in Limestone undergoing different dissolution regimes', *Transp Porous Med*, **101**, 507–532 (2014)

7. Nogues, Juan P., Fitts, Jeffrey P., Celia, Michael A. and Peters, Catherine A., Permeability evolution due to dissolution and precipitation of carbonates using reactive transport modeling in pore networks, *Water Resources Research*, **49(9)**, 6006–6021 (2013)

8. Van Noorden, T. L., Crystal precipitation and dissolution in a porous medium: effective equations and numerical experiments, Multiscale Model. Simul., **7(3)**, 1220–1236 (2009)

9. Parkhurst, D. and Appelo, C. Description of input and examples for phreeqc version 3—A computer program for speciation, batch-reaction, one-dimensional transport, and inverse geochemical calculations, U.S. Geological Survey Techniques and Methods, book 6, chap. A43, 497 p. (2013)

10. Pereira Nunes, J. P., Blunt, M. J. and Bijeljic, B. Pore-scale simulation of carbonate dissolution in micro-CT images, *Journal of Geophysical Research B: Solid Earth*, **121(2)**, 558–576, (2016)

11. Plummer, L. N., Wigley, T. M. L., Parkhurst, D. L., The kinetics of calcite dissolution in CO_2-water systems at 5° to 60°C and 0.0 to 1.0 ATM CO_2, *American Journal Of Science*, **278**, 179–216 (1978)

12. Plummer, L. N. and Busenberg, The solubilities

of calcite, aragonite and vaterite in CO_2-H_2O solutions between 0 and 90°C, and an evaluation of the aqueous model for the system $CaCO_3$-CO_2-H_2O, *Geochim. Cosmochim. Acta*, **46**, 1011–1040 (1982)

13. Roehl, P.O. and Choquette, P.W., Carbonate petroleum reservoirs, *Springer*, Intoduction (1985)

Acknowledgments

We acknowledge the support of the FOM-SHELL-CSER program (15CSER55 to PA and 14CSTT06 to JK and MW). This work is part of the research program of the Foundation for Fundamental Research of Matter (FOM), which is part of the Netherlands Organization for Scientific Research (NWO).